Biosensors and Bioelectronics 58 (2014) 1–8

Contents lists available at ScienceDirect

Biosensors and Bioelectronics

journal homepage: www.elsevier.com/locate/bios

Electrochemical displacement sensor based on ferrocene boronic acid tracer and immobilized glycan for saccharide binding proteins and *E. coli*

Decha Dechtrirat[a], Nenad Gajovic-Eichelmann[a,*], Felix Wojcik[b], Laura Hartmann[b], Frank F. Bier[a], Frieder W. Scheller[c,**]

[a] Fraunhofer Institute for Biomedical Engineering IBMT, Am Mühlenberg 13, 14476 Potsdam, Germany
[b] Max Planck Institute of Colloids and Interfaces, Am Mühlenberg 1, 14476 Potsdam, Germany
[c] Institute of Biochemistry and Biology, University of Potsdam, Karl-Liebknecht-Straße 24-25, 14476 Potsdam, Germany

ARTICLE INFO

Article history:
Received 22 November 2013
Received in revised form
11 February 2014
Accepted 11 February 2014
Available online 19 February 2014

Keywords:
Ferrocene benzoboroxol biosensor
Concanavalin A
Displacement
Escherichia coli
Ferrocene boronic acid
Self-assembled monolayer

ABSTRACT

Pathogens such as viruses and bacteria use their envelope proteins and their adhesin lectins to recognize the glycan residues presented on the cell surface of the target tissues. This principle of recognition is used in a new electrochemical displacement sensor for the protein concanavalin A (ConA). A gold electrode was first modified with a self-assembled monolayer of a thiolated mannose/OEG conjugate and a ferrocene boroxol derivative was pre-assembled as reporter molecule onto the mannose surface. The novel tracer molecule based on a 2-hydroxymethyl phenyl boronic acid derivative binds even at neutral pH to the saccharides which could expand the application towards biological samples (i.e., urine and feces). Upon the binding of ConA, the tracer was displaced and washed away from the sensor surface leading to a decrease in the electrochemical signal. Using square wave voltammetry (SWV), the concentration of ConA in the sample solution could be determined in the dynamic concentration range established from 38 nmol L^{-1} to 5.76 μmol L^{-1} with a reproducible detection limit of 1 μg mL^{-1} (38 nmol L^{-1}) based on the signal-to-noise ratio ($S/N=3$) with fast response of 15 min. The new reporter molecule showed a reduced non-specific displacement by BSA and ribonuclease A. The sensor was also successfully transferred to the first proof of principle for the detection of *Escherichia coli* exhibiting a detection limit of approximately 6×10^2 cells/mL. Specificity of the displacement by target protein ConA and *E. coli* was demonstrated since the control proteins (i.e., BSA and RNaseA) and the control *E. coli* strain, which lack of type 1 fimbriae, were ineffective.

1. Introduction

Rapid and sensitive detection of bacteria and their secreted toxins has become an urgent demand in the field of health care, environmental monitoring, food analysis, and security control to allow faster decisions to be made.

The commonly used receptors in biosensors for pathogen detection are based on antibodies and nucleic acids. During the past decade, carbohydrates have been increasingly considered as alternative bioreceptors because they are present on almost all cells as polysaccharides, glycolipids, glycoproteins, as well as other glycoconjugates and they are involved in many biological processes (Varki et al., 2009). In contrast to nucleic acids and antibodies, carbohydrates are more resistant against denaturation. Due to their small size, it is possible to have higher densities of carbohydrates per unit surface area. This high carbohydrate density will enable multivalent interactions which will enhance the binding affinity (Houseman and Mrksich, 2002). Mimicking the situations encountered on the cell surfaces during the initial recognition processes will offer a great promise to develop biosensors for the detection of carbohydrate binding proteins and pathogens.

For single step-detection, target-induced displacement is a promising format which has been reported so far for antibody based assays (Duarte et al., 2009), DNA (Mir and Katakis, 2008) and aptamer (Das et al., 2012; Feng et al., 2008; Hansen et al., 2006; Lu et al., 2008; Wu et al., 2007) based biosensors. To the best of our knowledge, the target-induced displacement of an electroactive tracer has not yet been applied so far in a sensor for the detection of lectins and *Escherichia coli*.

Boronic acid has been used for sugar recognition due to its ability to form a reversible covalent interaction with 1,2- and 1,3-cis-diols of the saccharides as 5- and 6-membered cyclic boronic esters,

* Corresponding author. Tel.: +49 331 58187 204; fax: +49 331 58187 119.
** Corresponding author. Tel.: +49 331 977 5121; fax: +49 331 977 5050.
E-mail addresses: nenad.gajovic@web.de (N. Gajovic-Eichelmann), fschell@uni-potsdam.de (F.W. Scheller).

http://dx.doi.org/10.1016/j.bios.2014.02.028
0956-5663

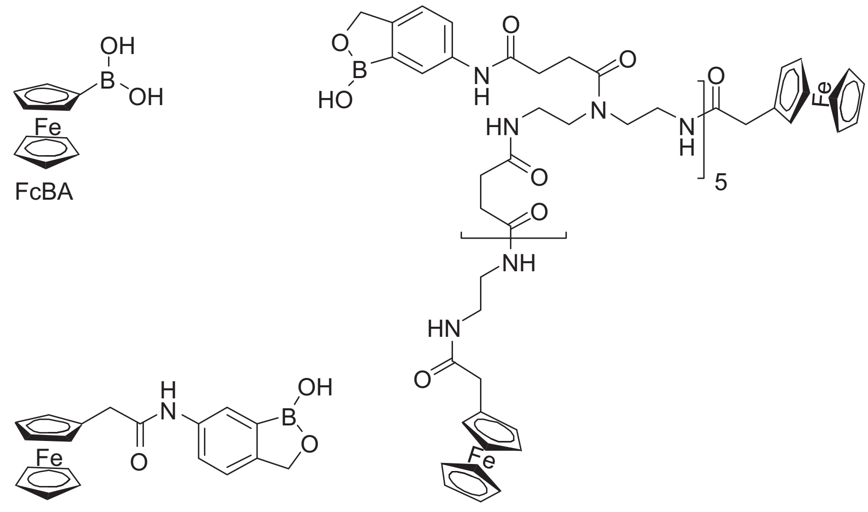

Fig. 1. Chemical structures of tracer molecules.

respectively. As a result it has been broadly used as recognition motif for sensing saccharides (Bull et al., 2013; Egawa et al., 2011; Wu et al., 2013). Among them the boronic acid based electrochemical sensors have been mostly reported. Since the boronic acid itself is electro-inactive in the useful potential range, it has been labeled with redox-active moieties such as ferrocene, tetrathiafluvalene (Shao and Zhao, 2010), and bipyridine Fe(II) complex (Nicolas et al., 2001). Ferrocene has been mostly used as an electrochemical reporter. FcBA (Fig. 1) is the simplest conjugate between boronic acid and ferrocene. In addition, it is also commercially available. Therefore, it has been intensively used in the previous reports for the electrochemical detection of sugars (Chien and Chou, 2011; Lacina and Skládal, 2011; Moore and Wayner, 1999; Norrild and Sotofte, 2002; Orl and Shinkai, 1995; Takahashi et al., 2011) and glycated molecules (i.e., lipopolysaccharide (Kato et al., 2007), glycosylated hemoglobin (Halámek et al., 2007; Liu et al., 2006)).

We demonstrate herein a new displacement sensor for the detection of saccharide binding proteins and *E. coli* based on the use of ferrocene boronic acid as an electroactive reporter molecule (Scheme 1). As proof of principle, interaction between Concanavalin A (ConA) and mannose is used. A gold electrode is first modified with a self-assembled monolayer (SAM) of a thiolated mannose/OEG conjugate followed by the pre-assembly of a ferrocene boronic acid derivative onto the mannose surface. Within this work three different kinds of tracers (Fig. 1) are studied and the results are compared. Upon the binding of the target protein to the mannose SAM, the tracer molecule is displaced and the decrease in the square wave voltammetry (SWV) signal can be correlated to the protein concentration in the sample solution. The sensor is also demonstrated for the detection of *E. coli*. Since it does not require a step after the addition of the target analyte, it is considered to be reagent-less and practical for on-site applications.

2. Materials and methods

2.1. Materials

Gold wire with a diameter of 0.5 mm was purchased from ChemPur (Germany) and 10 MHz AT-cut gold coated QCM sensor chips were purchased from 3T Analytik (Germany). Ferrocene boronic acid, ferroceneacetic acid, concanavalin A (ConA) from *Canavalia ensiformis*, ribonuclease A (RNaseA) from bovine pancreas, bovine serum albumin (BSA) and all other chemicals were purchased from Sigma-Aldrich (Germany) and were of analytical grade or higher. 5-Amino-2-hydroxymethylphenylboronic acid hydrochloride was purchased from Combi-Blocks (USA). *E. coli* strains DH5α and HB101 were obtained from Bio-Rad (Germany). All buffer salts were purchased from Roth (Germany). Ultrapure water from a laboratory water purification system (Sartorius, Germany) was used throughout this work.

2.2. Instruments

All electrochemical experiments were performed using a Gamry potentiostat Reference 600™ (Gamry Instruments, USA). A three-electrode system with a gold wire working electrode (10 mm length), a Pt wire counter electrode, and an Ag/AgCl (1 M KCl) reference electrode was used. All the real-time, label-free binding experiments were performed using a Gamry eQCM 10M (Gamry Instruments, USA).

2.3. Preparation and optimization of self assembled monolayers of thiolated linker and thiolated mannose/OEG conjugate

Prior to preparation of mannose modified surfaces, gold chip was cleaned using cold oxygen plasma for 10 min. Pure SAMs of Mann, ME, OEG1, and OEG2 were prepared by immersing the clean gold chip in 2 mM aqueous solution of each thiol. Mixed SAMs of Mann/ME, Mann/OEG1, and Mann/OEG2 were obtained by incubating the clean gold chip in binary mixture solution of Mann with ME, OEG1, or OEG2 at three different mole ratios (1:3, 2:2, and 3:1). The total concentration of thiol in each solution mixture was kept constant at 2 mM. The incubation was performed at room temperature for 3 h in phosphate buffered saline (PBS). After 3 h, the chip was thoroughly rinsed with water, gently dried under N_2 flow, and stored under Ar in the dark until measuring.

2.4. Preparation of the mannose modified surface

Prior to preparation of mannose modified surfaces, gold electrodes were cleaned using cold oxygen plasma for 10 min and subsequently electrochemical scanning in 0.1 M H_2SO_4 (from 0 to 1.5 V at a scan rate of 100 mV/s) until a stable cyclic voltammogram was obtained. The mixed SAM of Mann with OEG was prepared by immersing the gold electrodes in a 2 mM aqueous solution containing Mann and OEG with the mole ratio of 1:3 at room temperature for 3 h. After incubation, the electrodes were

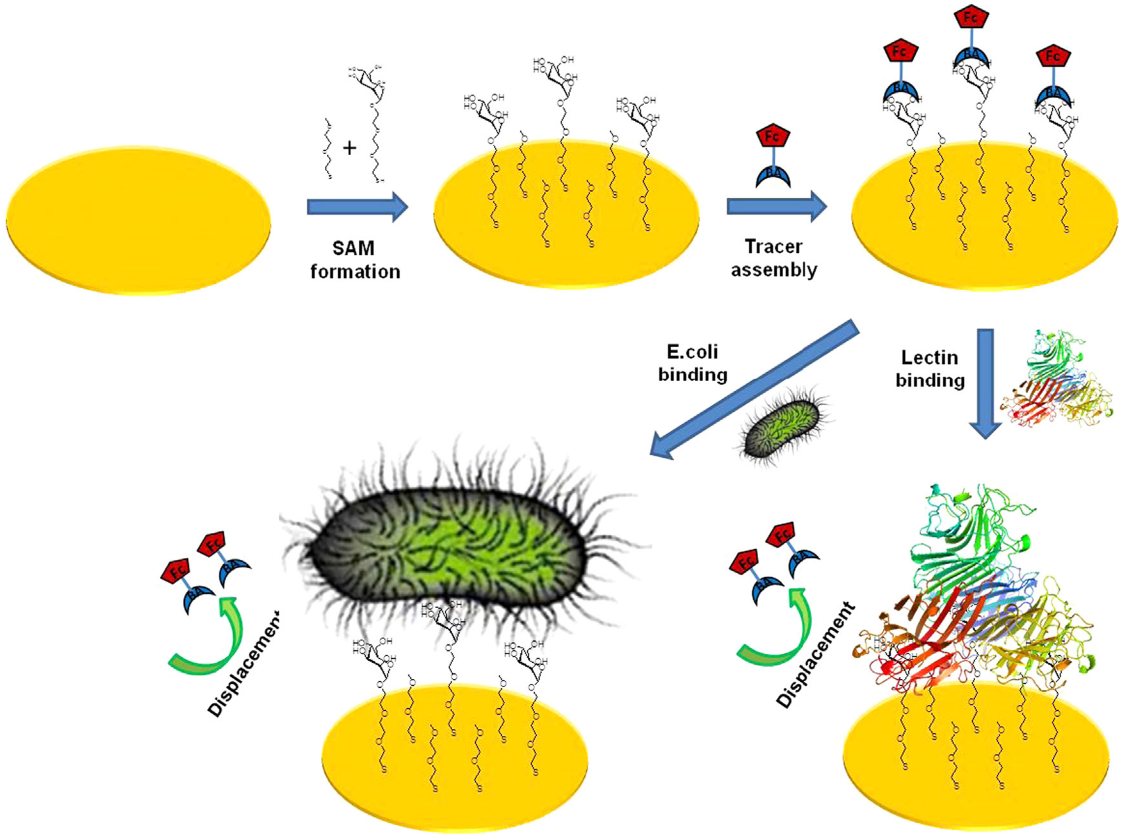

Scheme 1. Schematic representation of electrochemical displacement assay for carbohydrate binding protein and *E. coli* detection.

thoroughly rinsed with water, gently dried under N_2 flow, and stored under Ar. The electrodes were freshly prepared for each experiment.

2.5. Pre-assembly of the tracers

The 3 mM FcBA, 3 mM FcBZB, and 1 mg/mL Fc-pentaBZB solutions were freshly prepared in a mixture of 200 μL DMSO and 1800 μL buffers of different pH values. 100 mM phosphate buffer solutions of pH 6.0, 7.4, and 8.0 were prepared by mixing the stock standard solutions of K_2HPO_4 and KH_2PO_4, while 100 mM bicarbonate/carbonate buffer solutions of pH 9.2 and 10.3 were prepared by mixing the stock standard solutions of $NaHCO_3$ and Na_2CO_3. The mannose modified electrodes were incubated in 3 mM FcBA, 3 mM FcBZB, and 1 mg/mL Fc-pentaBZB solutions for 1 h. To remove the unbound tracers, the electrodes were gently washed with water for 30 s. To evaluate the amount of the surface-bound FcBA, FcBZB, and Fc-pentaBZB, square wave voltammetry (SWV) was carried out in 100 mM phosphate buffer (pH 7.4) by scanning the potential from −200 to 600 mV, with an increment of potential of 1 mV, at a frequency of 25 Hz and an amplitude of 25 mV. Baseline correction of the resulting voltammograms was performed and the peak current was recorded.

2.6. Displacement by proteins

After the pre-assembly step of the tracer molecule, the modified electrodes were incubated in a solution of ConA or in a binding buffer for 15 min. After the displacement, the electrodes were thoroughly rinsed with water and SWV was recorded. To verify the specificity of the displacement, the tracer bound electrodes were incubated in a solution of ConA, BSA, and RNaseA (100 μg/mL) for 15 min. To obtain the sensitivity of the assay, the tracer bound electrodes were incubated with varied concentration of ConA (over the range of 0.1–500 μg/mL) for 15 min. All solutions were prepared in 100 mM HEPES buffer (pH 7.4) containing 100 mM NaCl, 1 mM $MnCl_2$, and $CaCl_2$.

2.7. Displacement by E. coli

Two *E. coli* strains, DH5α and HB101, were cultured in LB broth at 37 °C for 24 h before use. After culturing, the bacteria were centrifuged, resuspended and washed with PBS buffer twice. Then they were sequentially diluted to the desired concentrations with PBS buffer. The concentration of *E. coli* in the stock solution was determined by measuring the optical density at 600 nm (OD600). To verify the specificity, the tracer bound electrodes were incubated in solutions of two *E. coli* strains (6×10^5 cells/mL) for 15 min. To attain the sensitivity, the tracer bound electrodes were incubated with varied concentrations of *E. coli* strain DH5α (over the range of 6×10^1–6×10^8 cells/mL) for 15 min. All solutions were prepared in PBS buffer. After the displacement, the electrodes were thoroughly rinsed with water and SWV was recorded.

2.8. Real-time rebinding studies using QCM

All measurements for the protein binding were performed in 100 mM HEPES buffer of pH 7.4 containing 100 mM NaCl, 1 mM $MnCl_2$, and $CaCl_2$ with a flow rate of 100 μL/min at 25 °C. For each measurement, the buffer was first injected for 10 min to attain a stable baseline and to reach equilibrium. ConA (over the range of 0.1–1000 μg/mL), BSA (100 μg/mL), and RNaseA (100 μg/mL) were used as the analytes to be investigated. The aqueous solutions of each protein were then injected for a contact time of 10 min. The protein free buffer was subsequently injected for 15 min. The report point, at which the binding response was assessed, was recorded at

25 min after the sample loading period. The binding of two *E. coli* strains DH5α and HB101 (6×10^8 cells/mL) was performed in PBS in the presence of 100 nmol L^{-1} of ConA with a flow rate of 100 μL/min at 25 °C for 25 min.

3. Results and discussion

3.1. Preparation and optimization of the mannose modified surface using QCM

In order to obtain the highest sensitivity of the sensors, surface chemistry of the mannose modified electrode must be optimized so that the binding of ConA reaches the highest response. To modulate this sugar/lectin interaction at the molecular level, the geometry, density, and environment of the surface-confined ligands are of great concern. The mannose probe was synthesized as a conjugate with a short oligoethylene glycol (OEG) and terminated with the thiol group (see Supporting information) and was termed as Mann hereafter. It is known that ConA displays selectivity for the α-configuration of mannose. Therefore, the mannose probe was designed to possess the α-glycosidic linkage. Since the sugar will be immobilized on the planar sensor surface, the sugar moiety must be displayed in a way that it is readily available for the binding while the non-specific adsorption to the modified surface or to the underlying metal transducer surface must be diminished. OEG has been broadly reported for its ability to suppress the non-specific adsorption of proteins (Lee and Laibinis, 1998; Prime and Whitesides, 1993). It has been therefore used as a spacer to improve the flexibility and to bring the mannose away from the surface by a linkage via a glycosidic bond (Guo et al., 2012; Min et al., 2010). To enhance the affinity of carbohydrate/lectin interactions, nature sums up weak monovalent binding by creating oligomeric forms of lectins. The simultaneous binding of multiple ligands to multiple recognition sites is termed as a multivalent interaction. To promote the multivalent sugar/protein interaction, a self-assembled monolayer (SAM) formation has been used for the preparation of a 2D-carbohydrate surface and the distance between ligands must fit the geometry of the tetrameric structure of ConA.

To modulate the density of the ligand, Mann is co-immobilized with three kinds of thiolated linkers including ME, OEG1, and OEG2 (Supporting information, Fig. S1A) as binary SAMs. The aim of using three different types of diluents with different length is to investigate the steric hindrance for the binding of ConA to the ligand. The optimization is carried out by preparing pure SAMs of Mann, ME, OEG1, and OEG2 as well as the binary mixed SAMs of Mann/ME, Mann/OEG1, and Mann/OEG2 at three different molar ratios (1:3, 2:2, and 3:1). Then binding of ConA to the resulting modified SAMs is characterized by the real-time measurements using quartz crystal microbalance (QCM) (Fig. S1B). The high mass change observed when ConA is exposed to the bare sensor electrode is obviously due to the non-specific adsorption of the protein to the bare metal surface. In case of a pure monolayer of Mann, the adsorption is assumed to reflect the specific interaction. However, the observed mass change is relatively low obviously because Mann is too densely packed so that binding of the large ConA is hindered. The surface density of Mann was then diluted using ME, OEG1, or OEG2 as diluents. ME is able to decrease the non-specific adsorption of ConA as compared to the bare electrode. However, ME is far too short and the SAM of short-chain thiol is known to be packed loosely containing pinholes and defects. Since ME itself shows pretty high non-specific adsorption, the observed responses of blended Mann/ME SAMs reflect both non-specific and specific adsorption making this system not selective enough for biosensing application. In contrast to ME, pure SAMs of OEG1 and OEG2 show very low mass changes expressing the low non-specific adsorption of ConA. Considering the mixed SAMs of Mann/OEG1 and Mann/OEG2, the highest binding capacities are obtained when 25% of Mann is mixed with 75% of OEG1 or OEG2. Increasing the percentage of Mann in the binary mixed SAMs results in reduction of protein binding which can be attributed to the steric crowding of the mannose ligand as the case of pure mannose SAM. The Mann/OEG2 shows better ConA binding than the mixed Mann/OEG1 SAM. This observation reveals that the length of the spacer used as the surface density modulator plays a big role in the accessibility of the surface bound sugar for the protein. As expected, the shorter OEG2 expresses less steric hindrance than the longer OEG1. With highest ConA binding capacity, the mixed SAM composed of Mann/OEG2 at the mole ratio of 1:3 is used in further experiments.

Cross-reactivity of the mannose surface against the control proteins (i.e., BSA and RNaseA) is shown in Fig. S2. The observed mass change of RNaseA on the mannose surface is almost negligible due to their lack of mannose binding sites. Although BSA is known as one of the most surface active proteins and frequently used as a surface blocking agent, its response to the mannose surface is nearly insignificant showing the high ability of OEG to suppress the non-specific adsorption.

The binding isotherm of ConA on the mannose surface is depicted in Fig. S3. By fitting the data with the Langmuir adsorption model, the dissociation constant (K_d) of 1.42 μM was obtained. This value is lower than that obtained from the monovalent mannose/ConA interaction by 2–3 orders of magnitude revealing the multivalent binding of ConA to the mannose surface (Che et al., 2010; Zheng and Du, 2013).

3.2. Tracers and preassembly of tracers

The tracer molecule is composed of two functionalities, namely ferrocene as an electroactive reporter module and boronic acid as a reversible sugar binding element. It is known that boronic acid forms a covalent interaction with 1,2- and 1,3-cis-diols as 5- and 6-membered cyclic boronic esters, respectively. However, this reaction is reversible and greatly influenced by the pH of the media. Therefore, it is very important to optimize the pH under which the preassembly of the tracer is carried out. To detect the tracer bound on the mannose modified electrode, square wave voltammetry (SWV) is chosen due to its high sensitivity towards the electrode bound redox probe. Within this work, three different derivatives of ferrocene boronic acid based tracer molecules (FcBA, FcBZB, and Fc-pentaBZB) are investigated (Fig. S4) and their responses on the electrode at different pH are depicted in Fig. 2.

The influence of pH during the preassembly of FcBA on the peak current of surface bound FcBA is shown in Fig. 2A. The peak current slightly increases between pH 6.0 and 7.0 and continues to increase up to pH 8.0 because the formation of the boronic ester bond between the unsubstituted arylboronic acid and diols is more favorable under alkaline conditions (James et al., 2006; Yan et al., 2004). This could be explained by the fact that under high hydroxide concentration, the hydroxide ion will coordinate with the electron-deficient boron atom and convert the less stable trigonal configuration of the boronic ester which is more readily reversible to the more stable tetrahedral conformation. However, the peak current abruptly drops off at the pH of 9.2 and 10.3 presumably due to the decomposition of Fc/Fc^+ in the presence of oxygen (Hurvois and Moinet, 2005; Zotti et al., 1998) under high basic condition (Breuer and Schmittel, 2012; Holecek et al., 1979) as confirmed by the precipitation of the reddish-brown gelatinous Ferric hydroxide from the solution. Therefore, the optimal pH value for the preassembly of FcBA onto the mannose surface is 8.0.

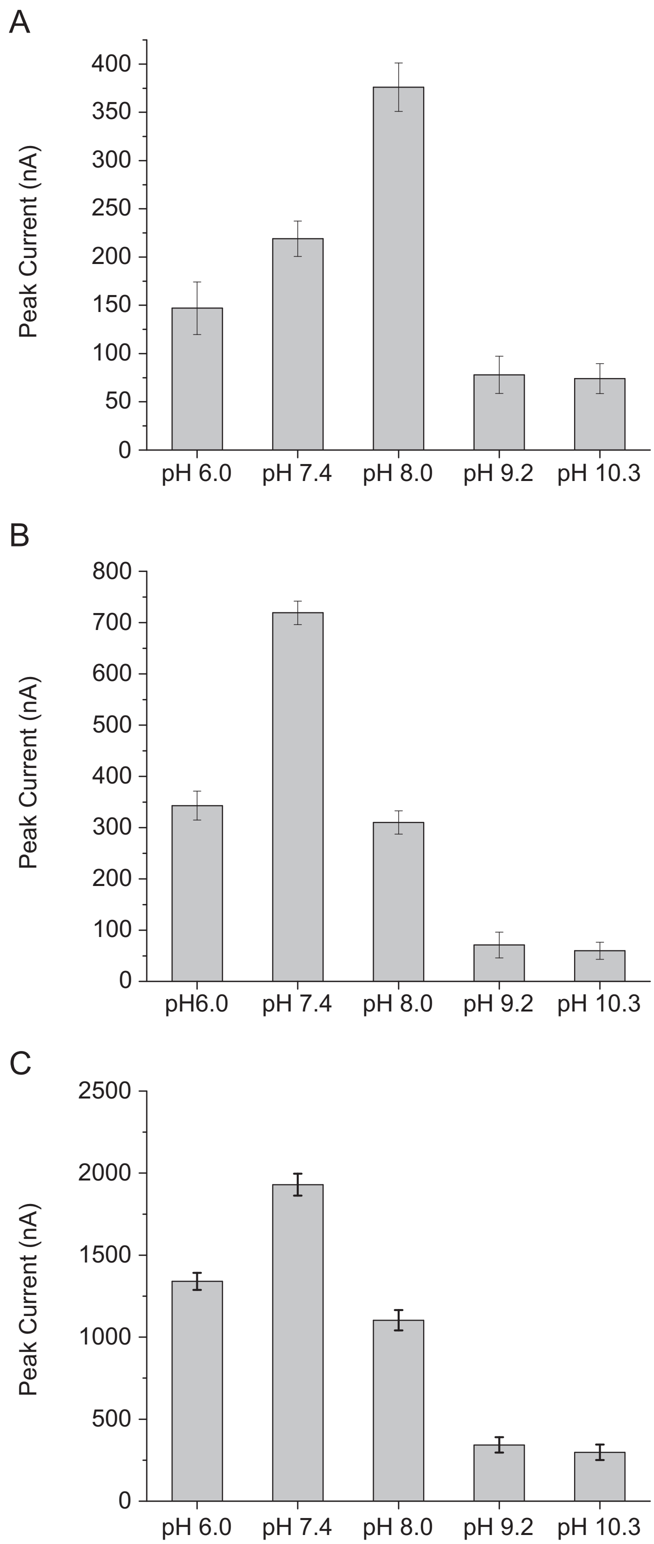

Fig. 2. Dependence of SWV peak current of the surface bound (A) FcBA, (B) FcBZB, and (C) Fc-pentaBZB on pH.

One major concern of using FcBA is its pH dependent binding equilibrium where the formation of the stable boronic ester bonds with many saccharides is favorable under alkaline conditions. This will limit the use of FcBA for biosensor applications especially when the physiological pH is required. To improve the sugar binding capability of boronic acid at milder pH, Hall and his colleagues (Bérubé et al., 2008) have modified the phenyl boronic acid by inserting the hydroxymethyl group at the ortho position close to the boron atom and termed as benzoboroxole (*o*-hydroxymethylphenylboronic acid). The resulting derivative has been proven to be able to bind to the sugar under the physiological pH due to the intramolecular interaction between B and O atoms which would stabilize the tetrahedral configuration of boron and prevent the hydrolysis of the boronic ester. To synthesize the tracer molecule which could bind to the sugar at the physiological pH (see Supporting information), an amino derivative of benzoboroxole was coupled to ferroceneacetic acid resulting in ferrocene benzoboroxole (FcBZB, Fig. 1). The preassembly of this new benzoboroxole based tracer to the mannose surface was carried out at different pH values and the peak current of the electrode bound FcBZB was depicted in Fig. 2B. As expected, the optimal binding of FcBZB was observed at the pH of 7.4 due to the favorable binding of benzoboroxole to the sugar under the physiological pH.

To increase the binding strength of the benzoboroxole based receptors, Hall and his colleagues (Pal et al., 2010) have inserted two benzoboroxole units onto the oligopeptide backbones while Kiser's group (Jay et al., 2010; Mahalingam et al., 2011) has coupled multiple units of benzoboroxole onto the linear polymeric chain. The resulting synthetic receptors have been proven to bind to their targets (TF antigen and gp120) with enhanced affinity via the multivalency effect. To increase the binding affinity of the tracer, a ferrocene terminated pentameric benzoboroxole functionalized on an oligo(amidoamine) (PAA) backbone (Fc-pentaBZB, Fig. 1) was synthesized using standard coupling and protecting group strategies for solid phase polymer synthesis. These novel monodisperse PAAs have been proven to be a powerful tool to modulate cellular behavior (Hartmann and Borner, 2009). To functionalize PAA backbones with benzoboroxole and ferrocene ligands several conjugation strategies such as thiol-ene chemistry (Wojcik et al., 2013a,b), Copper(I)-catalyzed Azide-Alkyne Cycloaddition (CuAAC) (Ponader et al., 2012) or amide bond formation (Wojcik et al., 2012) are feasible. In order to obtain a comparable linkage as reported for tracer FcBZB and to minimize the linker influence, here amide coupling chemistry on solid support was applied for the conjugation of the benzoboroxole units and amide coupling chemistry in solution after solid phase synthesis to attach the ferrocene ligands. Both amide bond formations are based on an elaborated protecting group protocol (Wojcik et al., 2012) using allyloxycarbonyl (Alloc) and *tert*-butyloxycarbonyl (Boc) protecting groups (for further details see Supporting information). Similar to FcBZB, Fc-pentaBZB also exhibits the maximal binding to the mannose surface at the physiological pH (Fig. 2C).

3.3. Displacement by proteins

After the preassembly of the tracer on the mannose modified electrode, the displacement of the tracer by the protein-free buffer and three different proteins including the target protein (ConA) as well as two controls (BSA and RNaseA) was performed. The SWV peak current of the remaining surface bound tracer was recorded and converted into a percentage of displacement taking into account that the signal from the preassembled tracer before the displacement is 100%. Non-specific displacement by the protein-free buffer was observed and was considered as a background signal. In case of FcBA (Fig. 3A), this background displacement of ca. 75% is as high as the displacement by ConA and two control proteins. This is mainly due to the fact that the displacement was performed at the physiological pH. Under such conditions, the boronic ester bond of FcBA is readily hydrolyzed leaving only tiny differentiation between specific and non-specific displacement. In contrast to FcBA, FcBZB binds stronger to the sugar at the pH of 7.4 which will lower the background displacement up to 50% as depicted in Fig. 3B. In this case, non-specific displacement by BSA

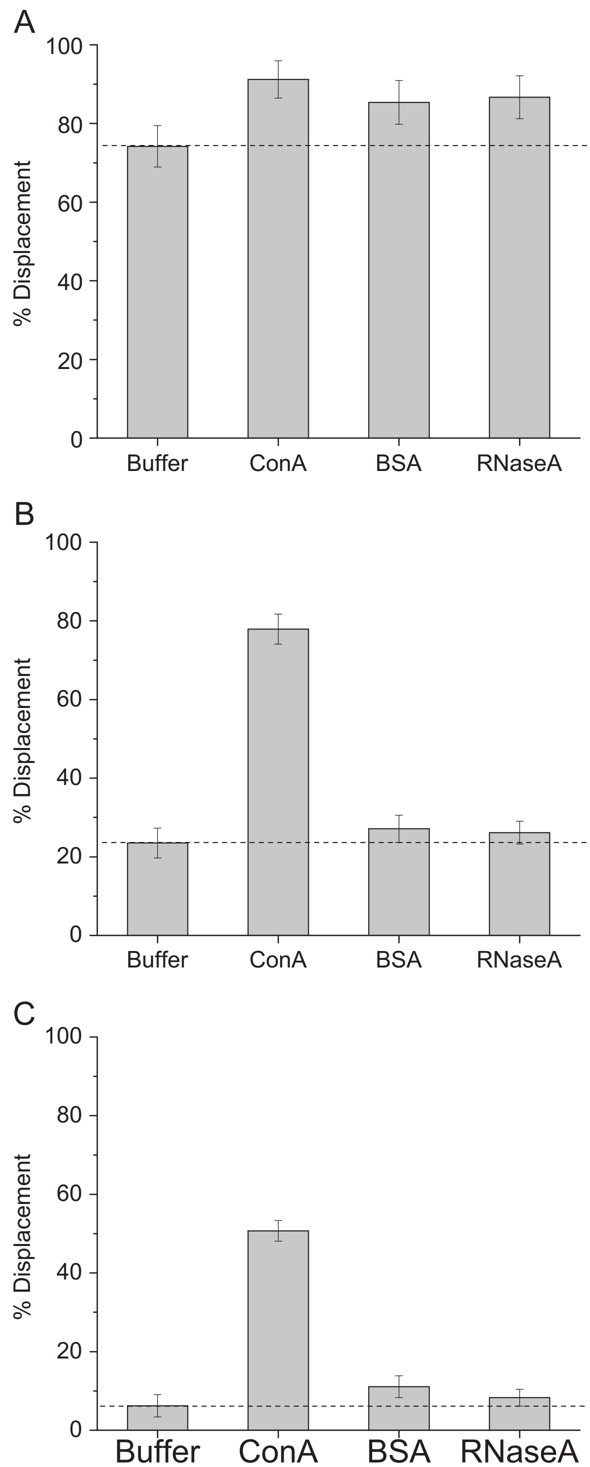

Fig. 3. Percentage of displacement of pre-assembled (A) FcBA, (B) FcBZB, and (C) Fc-pentaBZB by buffer, ConA, BSA, and RNaseA (at 100 μg mL^{-1} of each protein).

and RNaseA is comparable to the background signal but much lower than specific displacement by ConA. Due to its high discrimination between specific and non-specific displacement, FcBZB is considered as a promising reporter molecule for the sensor. With an attempt to enhance the stability of the tracer layer against the background dissociation, Fc-pentaBZB which bears five benzoboroxole units was synthesized and tested for its ability to differentiate the specificity of the displacement. As compared to FcBZB, the background signal of Fc-pentaBZB (Fig. 3C) is decreased by ca. 20% indicating that it binds much stronger than the monovalent tracer. In addition, it is also able to differentiate between the specific and non-specific displacement by the target protein and the controls, respectively. However, Fc-pentaBZB could only be partially displaced by ConA, even at high concentrations, thereby reducing the dynamic concentration range (data not shown). Obviously the binding affinity of Fc-pentaBZB to the surface was comparable to or higher than the binding affinity of ConA to the monosaccharide mannose. Therefore Fc-pentaBZB seems to be more suitable for the detection of higher affinity interactions, e.g. between some lectins and oligosaccharides. FcBZB was applied as the tracer for all further experiments, as it offered the best compromise between binding strength and dynamic concentration range.

The sensitivity of the sensor for ConA detection was evaluated by incubating the sensor with different concentrations of ConA. Fig. S5 shows SWV fast responses of the surface bound FcBZB after the displacement. The peak current decreases with increasing ConA concentrations. After converting the peak current into the percentage of displacement, a linear calibration plot in the concentration range of 0.038–5.76 μM was obtained (Fig. 4). A detection limit of 38 nM based on the signal-to-noise characteristics ($S/N=3$) could be achieved.

3.4. Displacement by *E. coli*

After the sensor has been successfully proven to be suitable for the detection of a model lectin (ConA), it was transferred to the detection of *E. coli*. It is known that 90% of urinary tract infections (UTI) are caused by *E. coli* and more than 95% of UTI-causing *E. coli* expresses type 1 fimbriae (Tchesnokova et al., 2011). The mannose specific binding is mediated by the adhesin protein FimH existing at the tip of the fimbriae (Klemm and Schembri, 2000; Krogfelt et al., 1990). Once the bacteria are able to enter the mammalian intestine, they will bind to the mannose containing sites on the epithelial cells via their fimbriae and will cause the infection. Within this work, two non-pathogenic strains of *E. coli* including DH5α and HB101 were selected and tested for the sensor. As confirmed in our QCM experiments (Fig. S6), DH5α binds to the modified mannose surface with high frequency change but HB101 shows only small response. In case of DH5α (Chart et al., 2000) it is clear that the binding to the mannose surface is caused by its type 1 fimbriae, while the lack of mannose binding ability of HB101 (Klemm et al., 1985) is mainly due to its defect in production of the type 1 fimbriae. Since the strain HB101 lacks the mannose binding adhesin, it serves as a good control to demonstrate that the binding of model *E. coli* (DH5α) does not come from the non-specific binding to the SAM layer. This result was also confirmed by the displacement sensor as shown in Fig. 5A. HB101 which does not bind to mannose shows very low non-specific displacement as compared to the background signal. In contrast, the strain DH5α which can specifically bind to the mannose modified electrode shows a complete displacement of the tracer at 6×10^5 cells/mL.

The sensor for the detection of *E. coli* strain DH5α was studied with concentrations of *E. coli* over the range of 6×10^1–6×10^8 cells/mL. The voltammograms of the surface bound FcBZB after the displacement by various concentrations of *E. coli* were depicted in Fig. S7 with the decreasing peak current while the *E. coli* concentrations increase. A linear relationship between the percentage of displacement and the logarithm of cell concentration was observed from 6×10^2 to 6×10^5 cells/mL as shown in Fig. 5B and the detection limit of 6×10^2 cells/mL based on the signal-to-noise ratio ($S/N=3$) was attained.

Limit of detections as well as the required measuring times from previous reports on biosensor based *E. coli* detection is summarized in Table S1. For the carbohydrate based biosensors, the limit of detection of our assay is comparable to that reported

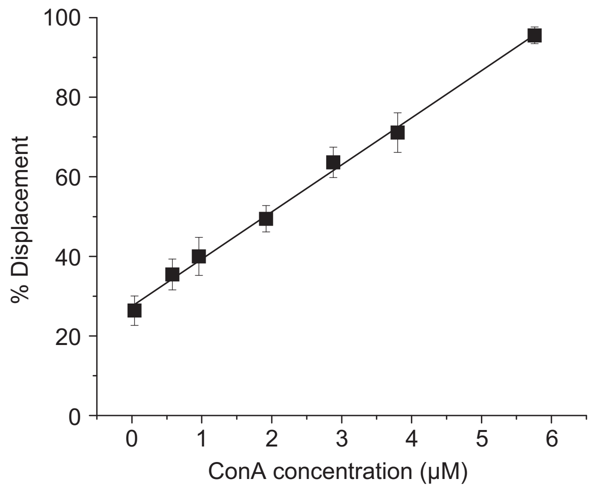

Fig. 4. Calibration curve for the detection of ConA.

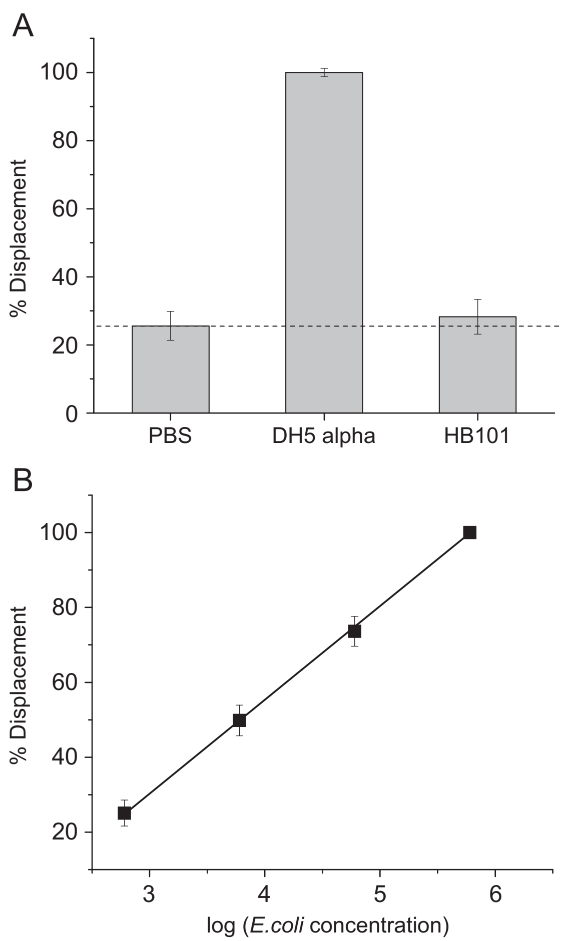

Fig. 5. (A) Percentage of displacement of pre-assembled FcBZB by buffer and *E. coli* strains DH5α and HB101 at 6×10^5 cells/mL. (B) Calibration curve for the detection of *E. coli* (DH5α).

by Guo et al. (2012) using electrochemical impedance spectroscopy (EIS) but much better than the QCM based technique reported by Shen et al. (2007). Our sugar based sensor obviously provides the same range of detection limit in comparison to other carbohydrate/lectin (Lu et al., 2009; Shen et al., 2007), DNA (Gau et al., 2001; Mao et al., 2006), and antibody (Campbell and Mutharasan, 2005; Su and Li, 2004) based sensors, while it offers better sensitivity as compared to other approaches which use lectins (Serra et al., 2008; Wang et al., 2013) as recognition elements. This clearly confirms the potential of carbohydrate modified sensing platforms as promising alternatives to the conventional antibody and nucleic acid based systems. Considering the detection time, our assay requires only 15 min which is much faster as compared to other reported protocols.

4. Conclusions

We have demonstrated a new electrochemical displacement sensor based on ferrocene boronic acid and immobilized mannose for saccharide binding proteins and *E. coli* detection. The redox active ferrocene boronic acid based tracer molecule is first pre-assembled onto mannose terminated SAM on the electrode surface. Upon the displacement by the target, the decrease of the electrochemical signal is detected and the concentration of the target analyte could be determined. Two new tracer molecules based on ortho-substituted phenylboronic acid known as benzoboroxole were synthesized which bind to the unprotected saccharides at physiological pH. This extends the application towards biological samples (i.e., urine and feces). The detection limits of the sensor towards ConA and *E. coli* are 1 μg mL^{-1} (38 nmol L^{-1}) and 6×10^2 cells/mL, respectively. Specificity of the displacement by target protein ConA and *E. coli* was demonstrated since the control proteins (i.e., BSA and RNaseA) and the control *E. coli* strain, which lack of type 1 fimbriae, were ineffective. In comparison to other methods, our sensor provides a fast analysis which could be completed within 15 min. Moreover, our assay is versatile and could be used for the detection of other carbohydrate binding proteins such as toxic plant lectins (i.e., ricin, abrin, and modeccin) or toxins secreted from bacteria (i.e., cholera toxin, shiga toxin, botulinum toxin, and tetanus toxin), as well as other pathogens (viruses and other bacteria) by altering the glycans. Since our sensor is reagent free and based on an uncomplicated electrochemical measurement, it could be further developed into a portable sensor device.

Acknowledgments

The authors gratefully acknowledge the financial support of BMBF (03IS2201A) of Germany, the Max Planck Society as well as the German Research Foundation (DFG, Emmy Noether program HA5950/1-1), and the Development and Promotion of Science and Technology Talents Project (DPST) by the Institute for the Promotion of Teaching Science and Technology (IPST). The authors also acknowledge Stefanie Arnold and Martina Obry (Fraunhofer IBMT, Golm) for the cultivation of *E. coli*.

Appendix A. Supporting information

Supporting information associated with this article can be found in the online version at http://dx.doi.org/10.1016/j.bios.2014.02.028.

References

Bérubé, M., Dowlut, M., Hall, D.G., 2008. J. Org. Chem. 73, 6471–6479.
Breuer, R., Schmittel, M., 2012. Organometallics 31, 1870–1878.
Bull, S.D., Davidson, M.G., Van Den Elsen, J.M.H., Fossey, J.S., Jenkins, A.T.A., Jiang, Y.B., Kubo, Y., Marken, F., Sakurai, K., Zhao, J., James, T.D., 2013. Acc. Chem. Res. 46, 312–326.
Campbell, G.A., Mutharasan, R., 2005. Biosens. Bioelectron. 21, 462–473.
Chart, H., Smith, H.R., La Ragione, R.M., Woodward, M.J., 2000. J. Appl. Microbiol. 89, 1048–1058.

Che, A.F., Huang, X.J., Xu, Z.K., 2010. Macromol. Biosci. 10, 955–962.
Chien, H.C., Chou, T.C., 2011. Electroanalysis 23, 402–408.
Das, J., Cederquist, K.B., Zaragozza, A.A., Lee, P.E., Sargent, E.H., Kelly, S.O., 2012. Nat. Chem. 4, 642–648.
Duarte, M.V., Lozano-Sanchez, P., Katakis, I., 2009. Biosens. Bioelectron. 24, 2205–2210.
Egawa, Y., Seki, T., Takahashi, S., Anzai, J.I., 2011. Mat. Sci. Eng. C 31, 1257–1264.
Feng, K., Sun, C., Kang, Y., Chen, J., Jiang, J.H., Shen, G.L., Yu, R.Q., 2008. Electrochem. Commun. 10, 531–535.
Gau, J.J., Lan, E.H., Dunn, B., Ho, C.M., Woo, J.C.S., 2001. Biosens. Bioelectron. 16, 745–755.
Guo, X., Kulkarni, A., Doepke, A., Halsall, H.B., Iyer, S., Heineman, W.R., 2012. Anal. Chem. 84, 241–246.
Halámek, J., Wollenberger, U., Stöcklein, W.F.M., Scheller, F.W., 2007. Electrochim. Acta 53, 1127–1133.
Hansen, J.A., Wang, J., Kawde, A.N., Xiang, Y., Gothelf, K.V., Collins, G., 2006. J. Am. Chem. Soc. 128, 2228–2229.
Hartmann, L., Borner, H.G., 2009. Adv. Mater. 21, 3425–3431.
Holecek, J., Handlir, K., Klikorka, J., Bang, N.D., 1979. Collect. Czechoslov. Chem. Commun. 44, 1379–1387.
Houseman, B.T., Mrksich, M., 2002. Top. Curr. Chem. 218, 1–44.
Hurvois, J.P., Moinet, C., 2005. J. Organomet. Chem. 690, 1829–1839.
James, T.D., Phillips, M.D., Shinkai, S., 2006. Boronic Acids in Saccharide Recognition. The Royal Society of Chemistry, Cambridge
Jay, J.I., Lai, B.E., Myszka, D.G., Mahalingam, A., Langheinrich, K., Katz, D.F., Kiser, P.F., 2010. Mol. Pharm. 7, 116–129.
Kato, D., Iijimi, S., Kurita, R., Sato, Y., Jia, J., Yabuki, S., Mizutani, F., Niwa, O., 2007. Biosens. Bioelectron. 22, 1527–1531.
Klemm, P., Jørgensen, B.J., van Die, I., de Ree, H., Bergmans, H., 1985. Mol. Gen. Genet. 199, 410–414.
Klemm, P., Schembri, M.A., 2000. Int. J. Med. Microbiol. 290, 27–35.
Krogfelt, K.A., Bergmans, H., Klemm, P., 1990. Infect. Immun. 58, 1995–1998.
Lacina, K., Skládal, P., 2011. Electrochim. Acta 56, 10246–10252.
Lee, S.W., Laibinis, P.E., 1998. Biomaterials 19, 1669–1675.
Liu, S., Wollenberger, U., Katterle, M., Scheller, F.W., 2006. Sens. Actuators B 113, 623–629.
Lu, Q., Lin, H., Ge, S., Luo, S., Cai, Q., Grimes, C.A., 2009. Anal. Chem. 81, 5846–5850.
Lu, Y., Zhu, N., Yu, P., Mao, L., 2008. Analyst 133, 1256–1260.
Mahalingam, A., Geonnotti, A.R., Balzarini, J., Kiser, P.F., 2011. Mol. Pharm. 8, 2465–2475.
Mao, X., Yang, L., Su, X.L., Li, Y., 2006. Biosens. Bioelectron. 21, 1178–1185.
Min, I.H., Choi, L., Ahn, K.S., Kim, B.K., Lee, B.Y., Kim, K.S., Choi, H.N., Lee, W.Y., 2010. Biosens. Bioelectron. 26, 1326–1331.
Mir, M., Katakis, I., 2008. Talanta 75, 432–441.
Moore, A.N.J., Wayner, D.D.M., 1999. Can. J. Chem. 77, 681–686.
Nicolas, M., Fabre, B., Simonet, J., 2001. Electrochim. Acta 46, 1179–1190.
Norrild, J.C., Sotofte, I., 2002. J. Chem. Soc. Perkin Trans. 2, 303–311.
Orl, A., Shinkai, S., 1995. J. Chem. Soc. Chem. Commun., 1771–1772
Pal, A., Bérubé, M., Hall, D.G., 2010. Angew. Chem. Int. Ed. 49, 1492–1495.
Ponader, D., Wojcik, F., Beceren-Braun, F., Dernedde, J., Hartmann, L., 2012. Biomacromolecules 13, 1845–1852.
Prime, K.L., Whitesides, G.M., 1993. J. Am. Chem. Soc. 115, 10714–10721.
Serra, B., Gamella, M., Reviejo, A.J., Pingarrón, J.M., 2008. Anal. Bioanal. Chem. 391, 1853–1860.
Shao, M., Zhao, Y., 2010. Tetrahedron Lett. 51, 2508–2511.
Shen, Z., Huang, M., Xiao, C., Zhang, Y., Zeng, X., Wang, P.G., 2007. Anal. Chem. 79, 2312–2319.
Su, X.L., Li, Y., 2004. Biosens. Bioelectron. 19, 563–574.
Takahashi, S., Abiko, N., Haraguchi, N., Fujita, H., Seki, E., Ono, T., Yoshida, K., Anzai, J.I., 2011. J. Environ. Sci. 23, 1027–1032.
Tchesnokova, V., Aprikian, P., Kisiela, D., Gowey, S., Korotkova, N., Thomas, W., Sokurenko, E., 2011. Infect. Immun. 79, 3895–3904.
Varki, A., Cummings, R.D., Esko, J.D., Freeze, H.H., Stanley, P., Bertozzi, C.R., Hart, G.W., Etzler, M.E., 2009. Essentials of Glycobiology, second ed. Cold Spring Harbor, New York
Wang, Y., Ye, Z., Si, C., Ying, Y., 2013. Food Chem. 136, 1303–1308.
Wojcik, F., Lel, S., O'Brien, A.G., Seeberger, P.H., Hartmann, L., 2013a. Beilstein J. Org. Chem. 9, 2395–2403.
Wojcik, F., Mosca, S., Hartmann, L., 2012. J. Org. Chem. 77, 4226–4234.
Wojcik, F., O'Brien, A.G., Götze, S., Seeberger, P.H., Hartmann, L., 2013b. Chem. Eur. J. 19, 3090–3098.
Wu, X., Li, Z., Chen, X.X., Fossey, J.S., James, T.D., Jiang, Y.B., 2013. Chem. Soc. Rev. 42, 8032–8048.
Wu, Z.S., Guo, M.M., Zhang, S.B., Chen, C.R., Jiang, J.H., Shen, G.L., Yu, R.Q., 2007. Anal. Chem. 79, 2933–2939.
Yan, J., Springsteen, G., Deeter, S., Wang, B.H., 2004. Tetrahedron 60, 11205–11209.
Zheng, H., Du, X., 2013. Biochim. Biophys. Acta 1828, 792–800.
Zotti, G., Schiavon, G., Zecchin, S., Favretto, D., 1998. J. Electroanal. Chem. 456, 217–221.